SERCA pump activity is physiologically regulated by presenilin and regulates amyloid β production

Kim N. Green, Angelo Demuro, Yama Akbari, Brian D. Hitt, Ian F. Smith, Ian Parker, and Frank M. LaFerla

Department of Neurobiology and Behavior, University of California, Irvine, Irvine, CA 92697

In addition to disrupting the regulated intramembraneous proteolysis of key substrates, mutations in the presenilins also alter calcium homeostasis, but the mechanism linking presenilins and calcium regulation is unresolved. At rest, cytosolic Ca^{2+} is maintained at low levels by pumping Ca^{2+} into stores in the endoplasmic reticulum (ER) via the sarco ER Ca^{2+}-ATPase (SERCA) pumps. We show that SERCA activity is diminished in fibroblasts lacking both PS1 and PS2 genes, despite elevated SERCA2b steady-state levels, and we show that presenilins and SERCA physically interact. Enhancing presenilin levels in *Xenopus laevis* oocytes accelerates clearance of cytosolic Ca^{2+}, whereas higher levels of SERCA2b phenocopy PS1 overexpression, accelerating Ca^{2+} clearance and exaggerating inositol 1,4,5-trisphosphate–mediated Ca^{2+} liberation. The critical role that SERCA2b plays in the pathogenesis of Alzheimer's disease is underscored by our findings that modulating SERCA activity alters amyloid β production. Our results point to a physiological role for the presenilins in Ca^{2+} signaling via regulation of the SERCA pump.

Introduction

PS1 and PS2 are highly conserved integral membranous proteins that localize predominantly to the ER. Mutations in the PS1 and PS2 genes that cause autosomal-dominant early-onset Alzheimer's disease (AD) disrupt several cellular pathways, including altered γ-secretase–mediated cleavage of the amyloid precursor protein (APP) to form amyloid β (Aβ) peptides (Duff et al., 1996) and disruption of intracellular Ca^{2+} homeostasis (LaFerla, 2002; Demuro et al., 2005). Ca^{2+} signaling disruptions manifest as enhanced filling of ER Ca^{2+} stores (Leissring et al., 1999b), attenuation of capacitive Ca^{2+} entry stores (Leissring et al., 2000; Yoo et al., 2000; Smith et al., 2002; Herms et al., 2003), and by exaggerated liberation of Ca^{2+} from the ER by the second messenger inositol 1,4,5-trisphosphate (IP_3; Leissring et al., 1999b; Yoo et al., 2000; Smith et al., 2002; Stutzmann et al., 2004). Given that mutations in presenilin disrupt intracellular Ca^{2+} signaling, we set out to determine whether presenilins may serve a physiological role in intracellular Ca^{2+} homeostasis.

In support of a role in Ca^{2+} homeostasis, overexpression of wild-type PS1 or PS2 in *Xenopus laevis* oocytes causes enhanced IP_3-mediated Ca^{2+} release, an effect that is exacerbated by mutations in both genes (Leissring et al., 1999b). However, it remains unclear whether the exaggerated IP_3-evoked responses result from modulation of the IP_3 signaling pathway, such as sensitization of IP_3 receptors by presenilins, or as a consequence of overfilling of ER stores. Recently, the presenilins have been reported to be able to form ER leak channels, and it has been reported that mutations in the presenilins disrupt this function (Tu et al., 2006). However, it is unclear how leak channel formation could account for the numerous reports of wild-type presenilin overexpression increasing IP_3-mediated calcium release.

Ca^{2+} pumps, along with Ca^{2+} release channels, are the key components of Ca^{2+} regulatory systems in neuronal and non-neuronal cells (Berridge et al., 2000). The sarco ER Ca^{2+}-ATPase (SERCA) pumps have the highest affinity for Ca^{2+} removal from the cytosol and, together with plasma membrane Ca^{2+}-ATPases and transporters, determine the resting cytosolic Ca^{2+} concentration. Three differentially expressed genes encode at least five isoforms of the SERCA pump. SERCA1a and -1b are expressed in skeletal muscle, whereas SERCA2a is expressed in cardiac muscle (Aubier and Viires, 1998). SERCA2b, which has a C-terminal extension, is ubiquitously expressed in smooth muscle tissues and nonmuscle tissues including neurons (Baba-Aissa et al., 1998). SERCA3 has limited expression in various nonmuscle tissues (Baba-Aissa et al., 1998).

K.N. Green and A. Demuro contributed equally to this paper.

Correspondence to Frank M. LaFerla: laferla@uci.edu

Abbreviations used in this paper: Aβ, amyloid β; AD, Alzheimer's disease; AICD, APP intracellular domain; APP, amyloid precursor protein; CCE, capacitative Ca^{2+} entrance; FAD, familial AD; IP_3, inositol 1,4,5-trisphosphate; MEF, mouse embryonic fibroblast; nAChR, nicotinic acetylcholine receptor; pcDNA, pseudo-cDNA; PSDKO, presenilin double knockout; SERCA, sarco ER Ca^{2+}-ATPase.

The online version of this paper contains supplemental material.

The Rockefeller University Press $30.00
J. Cell Biol. Vol. 181 No. 7 1107–1116
www.jcb.org/cgi/doi/10.1083/jcb.200706171

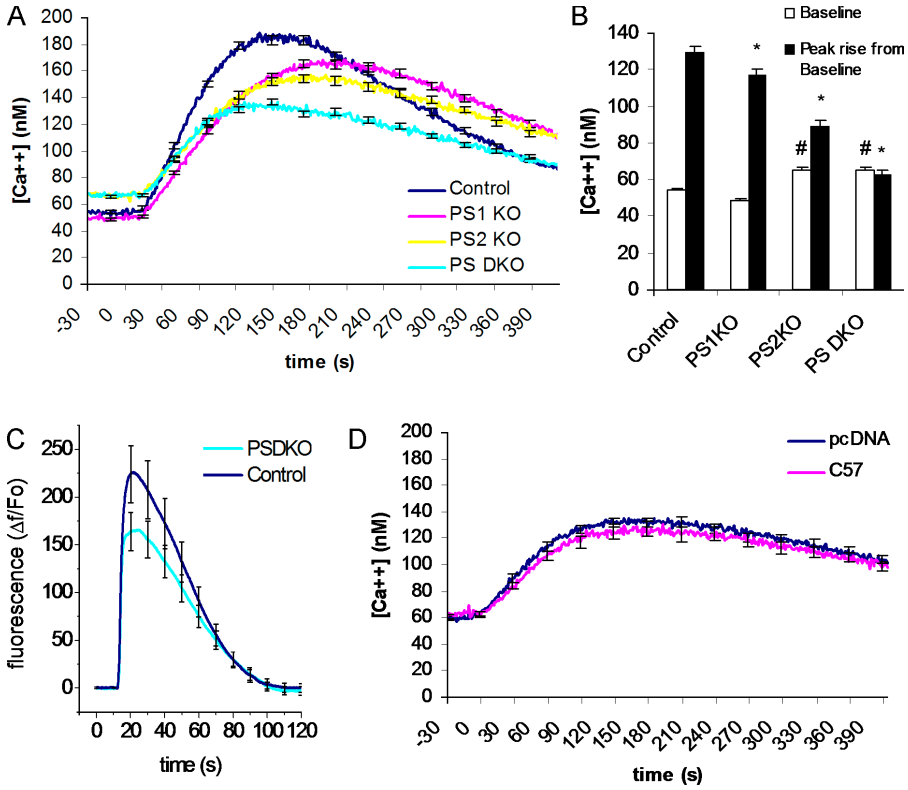

Figure 1. **Elevated cytosolic Ca^{2+} and reduced ER Ca^{2+} stores in presenilin-null cell line.** (A) Changes in cytosolic Ca^{2+} evoked by thapsigargin in control fibroblasts (control; *n* = 48 cells) and fibroblasts from PSDKO (*n* = 57 cells), PS1KO (*n* = 48), and PS2KO (*n* = 56) mice. ER Ca^{2+} stores were released into the cytosol by application of 1 μM thapsigargin, a specific blocker of SERCA activity, with 0 mM Ca^{2+} in the bathing solution. Basal cytosolic Ca^{2+} levels were elevated (~70 nM) in the PSDKO and PS2KO fibroblasts compared with controls and PS1KO cells (~50 nM; $P < 0.05$), whereas the peak Ca^{2+} signals after application of thapsigargin were substantially reduced in PSDKO and PS2KO fibroblasts. (B) Mean values of basal cytosolic [Ca^{2+}] and thapsigargin-evoked Ca^{2+} signals, derived from the experiments in A. *, significance in peak rise versus pcDNA ($P < 0.05$); #, significance in basal levels versus pcDNA ($P < 0.05$). (C) Changes in cytosolic Ca^{2+} evoked by 1 μM ionomycin in control fibroblasts (control; *n* = 12 cells) and fibroblasts from PSDKO mice (*n* = 37 cells), with 0 mM Ca^{2+} in the bathing solution. (D) Cytosolic Ca^{2+} signals in PSDKO fibroblasts transfected either with pcDNA (*n* = 63 cells) or AICD (*n* = 54 cells) 48 h earlier. No significant differences were apparent in either basal cytosolic Ca^{2+} levels or the peak response after application of 1 μM thapsigargin. Error bars show SEM.

Given that overfilled ER Ca^{2+} stores are one consequence of most PS1 mutations, we hypothesized that presenilin may regulate SERCA pump activity. In this paper, we used both gain-of-function and loss-of-function genetic approaches to show that presenilins are required for proper functioning of SERCA activity in both mammalian cell lines and *X. laevis* oocytes. Notably, we find that presenilins physically associate with SERCA, and modulation of SERCA function via genetic or pharmacological means results in altered Aβ production. Furthermore, SERCA2b knockdown mimics the Ca^{2+} dynamics seen in presenilin-null cells. Collectively, these results suggest that presenilins regulate and are necessary for normal functioning of the SERCA2b pump, most likely through a direct protein–protein interaction, and that SERCA activity itself impacts Aβ generation.

Results

Elevated cytosolic Ca^{2+} levels and attenuated ER Ca^{2+} stores in presenilin-null cells

We previously showed that presenilin mutations lead to enhanced filling of ER Ca^{2+} stores (Leissring et al., 1999a,b). To further explore the role of endogenous presenilin in intracellular Ca^{2+} signaling, we investigated ER Ca^{2+} stores in immortalized mouse embryonic fibroblast (MEF) cells from presenilin double-knockout (PSDKO) mice (Herreman et al., 1999). Cytosolic Ca^{2+} signals were recorded in Fura-2-AM–loaded cells before and during stimulation with 1 μM thapsigargin, a potent irreversible inhibitor of the SERCA pump (Lytton et al., 1991).

PSDKO fibroblasts displayed elevated resting cytosolic Ca^{2+} levels compared with control cells (Fig. 1, A and B). Application of thapsigargin in the bath perfusion promoted a transient rise of cytosolic [Ca^{2+}] signal as a consequence of constitutively active Ca^{2+} leakage from the ER, providing a signal proportional to the amount of Ca^{2+} sequestered in the ER, although it does not take into account differences in Ca^{2+} efflux across the plasma membrane. PSDKO fibroblasts showed reduced responses to thapsigargin as compared with control fibroblasts (Fig. 1 B). These results are consistent with diminished SERCA activity, as it is this ER Ca^{2+} pump which helps to maintain low cytosolic resting Ca^{2+} level by actively pumping Ca^{2+} from the cytosol into the ER stores, thereby regulating the Ca^{2+} levels between the two compartments.

To determine the respective contribution of the two presenilins, we next investigated Ca^{2+} responses in PS1-deficient (PS1KO) or PS2-deficient (PS2KO) fibroblasts. Basal cytosolic Ca^{2+} levels were elevated in the PS2KO cells at comparable levels to those observed in the PSDKO fibroblasts. Likewise, the PS2KO cells also showed diminished responses after treatment with thapsigargin. In contrast, the PS1KO cells showed small or no changes in basal Ca^{2+} levels but did show diminished thapsigargin-mediated responses (Fig. 1, A and B). Therefore, although both PS1 and 2 appear to regulate intracellular Ca^{2+} homeostasis, it appears to be PS2 that plays a larger role in maintaining low cytosolic Ca^{2+} levels and appropriate filling of ER Ca^{2+} stores. We next looked at ionomycin-evoked calcium release in control and PSDKO cells (Fig. 1 C). Ionomycin is an ionophore that causes the release of Ca^{2+} from most intracellular stores. Application of 1 μM ionomycin in the absence of extracellular Ca^{2+} evoked smaller rises and areas

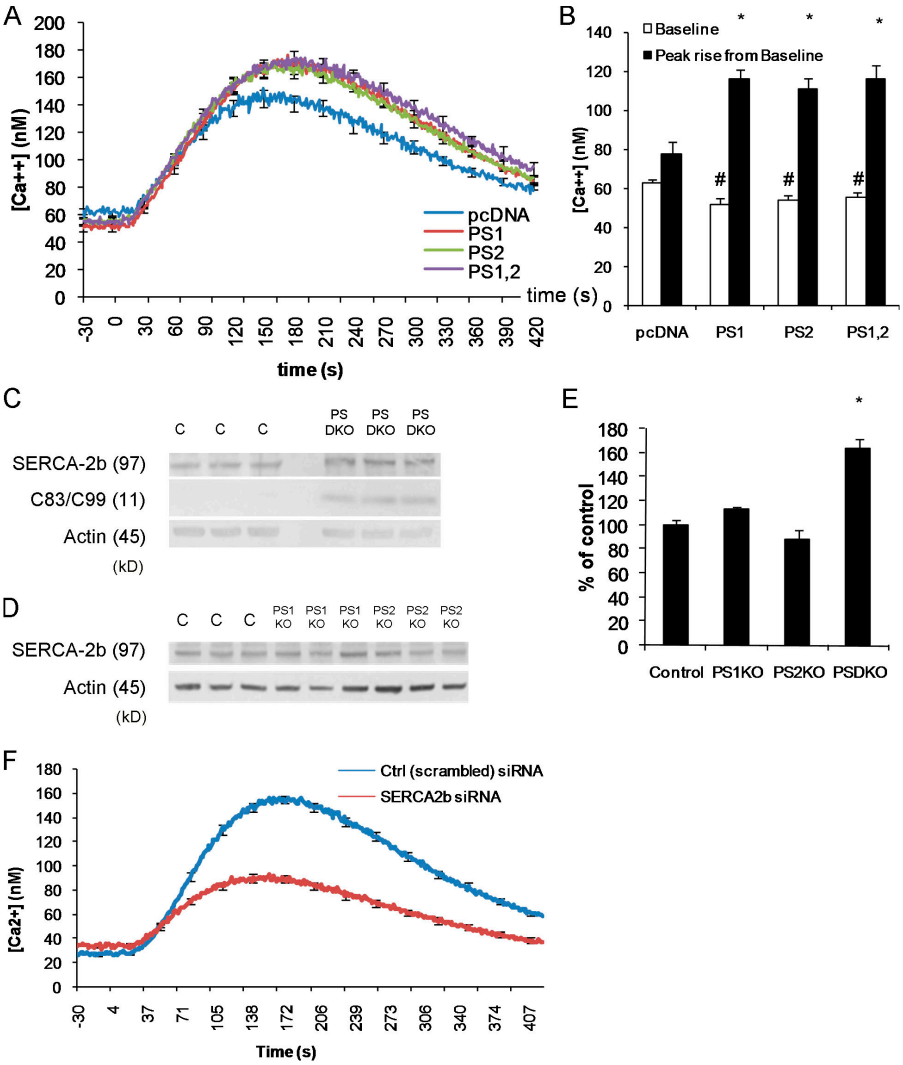

Figure 2. **Ca^{2+} deficits in presenilin-null fibroblasts are not caused by reduced SERCA2b expression.** (A) Changes in cytosolic Ca^{2+} evoked by thapsigargin in PSDKO fibroblasts transfected 48 h earlier with pcDNA (n = 25 cells), PS1 (n = 40 cells), PS2 (n = 48 cells), or both PS1 and 2 (n = 47 cells), with 0 mM Ca^{2+} in the bathing solution. Basal cytosolic Ca^{2+} levels were reduced (~20 nM) in the presenilin-transfected fibroblasts compared with controls, whereas the peak Ca^{2+} signals after application of thapsigargin were significantly increased in presenilin-transfected fibroblasts. (B) Mean values of basal cytosolic Ca^{2+} and thapsigargin-evoked Ca^{2+} signals, derived from the experiments in A. *, significance in peak rise versus pcDNA ($P < 0.05$); #, significance in basal levels versus pcDNA ($P < 0.05$). (C) Steady-state levels of SERCA2b protein are higher in PSDKO fibroblasts compared with controls based on Western blotting. The PSDKO fibroblasts also displayed C83–C99 APP fragments that were not present in the controls because of the lack of γ-secretase activity. β-Actin levels are shown as a loading control. (D) Steady-state levels of SERCA2b in PS1KO and PS2KO fibroblasts compared with controls based on Western blotting. (E) Densitometric analysis of the SERCA2b levels in C and D, normalized to β-actin, showing elevation of SERCA2b levels in the PSDKO fibroblasts. *, significance in peak rise versus pcDNA ($P < 0.05$; n = 3). (F) Genetic down-regulation of SERCA2b expression lowers ER Ca^{2+} stores and elevates basal Ca^{2+} levels. siRNA-mediated down-regulation of SERCA2b leads to lower ER Ca^{2+} stores (*, $P < 0.001$; n = 105 cells) when compared with cells treated with a control (scrambled) siRNA. Error bars show SEM.

under the curve (9,425 vs. 7,394 fluorescent units) from the PSDKO cells compared with the controls.

The presenilins are an integral part of the γ-secretase complex that is responsible for cleavage of the C99 fragment of APP to form Aβ and the APP intracellular domain (AICD). Cells lacking presenilins do not have γ-secretase activity and consequently produce no Aβ or AICD (Zhang et al., 2000; Hass and Yankner, 2005). Because the absence of the AICD region of APP has been shown to cause deficits in Ca^{2+} release from ER stores (Leissring et al., 2002), we sought to determine whether the Ca^{2+} dyshomeostasis in PSDKO cells could be attributed to lack of AICD production rather than to the absence of presenilins themselves. For this purpose, PSDKO fibroblasts were transfected with the AICD (C57) fragment and compared with control pseudo-cDNA (pcDNA)–transfected PSDKO fibroblasts. However, even after 48 h of incubation to allow expression of AICD (Fig. 1 D), control and AICD-expressing PSDKO fibroblasts showed no significant differences in basal or thapsigargin-evoked Ca^{2+} levels. Given that overexpression of AICD into PSDKO cells did not recover either basal or thapsigargin-evoked Ca^{2+} levels, we then overexpressed PS1, PS2, or both together in PSDKO cells. Overexpression of either PS1, PS2, or both together rescued both the basal and thapsigargin-evoked Ca^{2+} levels to the same degree (Fig. 2, A and B).

SERCA2b steady-state levels are elevated in presenilin-null cells

The observed phenotype of elevated basal cytosolic Ca^{2+} and reduced ER Ca^{2+} store content in presenilin-null cells is consistent with either reduced levels of SERCA2b or a reduction in functional activity of SERCA pumps (Zhang et al., 2006). Surprisingly, we found that SERCA2b steady-state levels, the isoform of SERCA found in brain neurons, were elevated, rather than diminished, in the PSDKO fibroblasts (Fig. 2, C and E), suggesting that SERCA activity was impaired in the absence of presenilins and that the cells attempt to compensate by increasing SERCA expression. The presence of either PS1 or 2 is sufficient to prevent this increase in SERCA2b steady-state levels as shown in PS1KO and PS2KO cell lines (Fig. 2, D and E). Given our hypothesis that SERCA activity was impaired in the absence of presenilin, we attempted to mimic the Ca^{2+} phenotype seen in PSDKO cells via siRNA knockdown of SERCA2b in CHO cells. Knockdown of SERCA2b levels resulted in elevated basal Ca^{2+} levels, and a marked decrease in thapsigargin evoked Ca^{2+} release (Fig. 2 F).

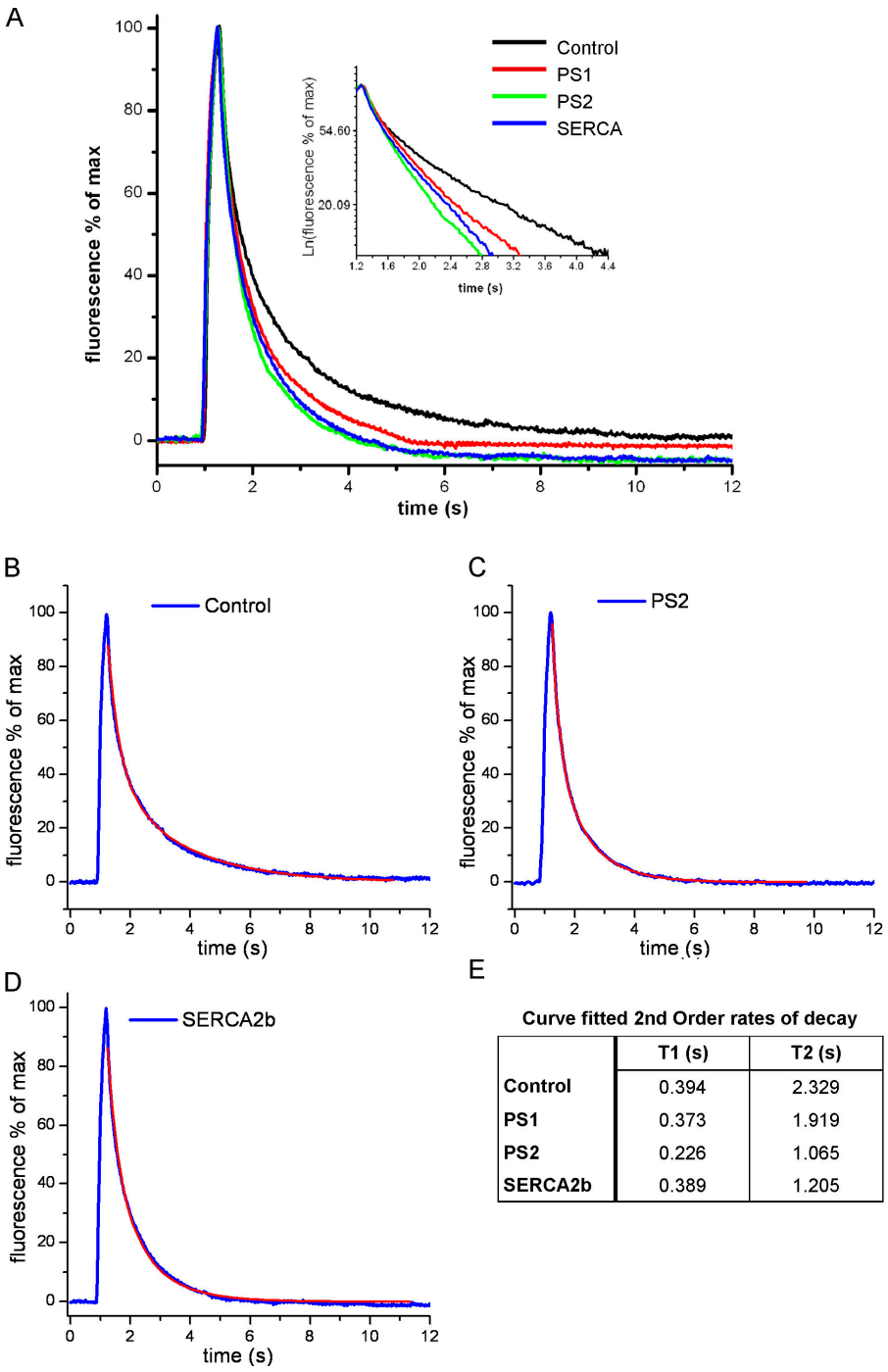

Figure 3. **PS1 and PS2 accelerate the clearance of cytosolic Ca^{2+} after entry via muscle nAChR channels.** (A) Ca^{2+}-dependent fluorescence changes ($\Delta F/F_o$) after 300-ms hyperpolarizing pulses to induce Ca^{2+} entry through nAChR expressed in the plasma membrane. Traces show mean data from >35 recordings in multiple oocytes injected 3 d earlier with αβδγ nAChR subunits alone (control) or together with PS1, PS2, or SERCA2b cRNA. The inset shows the same data on a semilogarithmic scale. (B–D) Data from, respectively, control, PS2, and SERCA2b oocytes, fitted by biexponential decays (superimposed red traces). (E) Table listing fast (T1) and slow (T2) time constants of double-exponential fits to the Ca^{2+} decay data.

This phenotype was remarkably similar to that seen in the PS-DKO cell line, giving further credence to presenilin regulation of SERCA function. It should be noted that it is unlikely that changes in SERCA function directly modulate basal cytosolic Ca^{2+} levels but that they probably do so through changes in other Ca^{2+} influx pathways such as store-operated Ca^{2+} entry.

PS1 and PS2 mimic SERCA2b-accelerated cytosolic Ca^{2+} clearance

Based on these data from presenilin-null cell lines, we moved to a more regulatable system to directly establish whether presenilins modulate SERCA pump activity. We used the *X. laevis* oocyte expression system to monitor the clearance of Ca^{2+} ions from the cytosol after a transient influx across the plasma membrane. For this purpose, oocytes were induced to express the Ca^{2+}-permeable nicotinic acetylcholine receptor (nAChR) that served as a "Ca^{2+} switch," allowing precisely controlled cytosolic Ca^{2+} transients to be evoked by pulsing the membrane potential to strongly negative voltages to increase the electrochemical driving force for Ca^{2+} entry. Oocytes were loaded with the Ca^{2+}-sensitive dye Oregon Green BAPTA 1 and were voltage-clamped at a holding potential of 0 mV to minimize Ca^{2+} influx. In the presence of 100–500 nM acetylcholine, a brief (300 ms) hyperpolarizing pulse to −150 mV produced a transient Ca^{2+} fluorescence signal because of Ca^{2+}

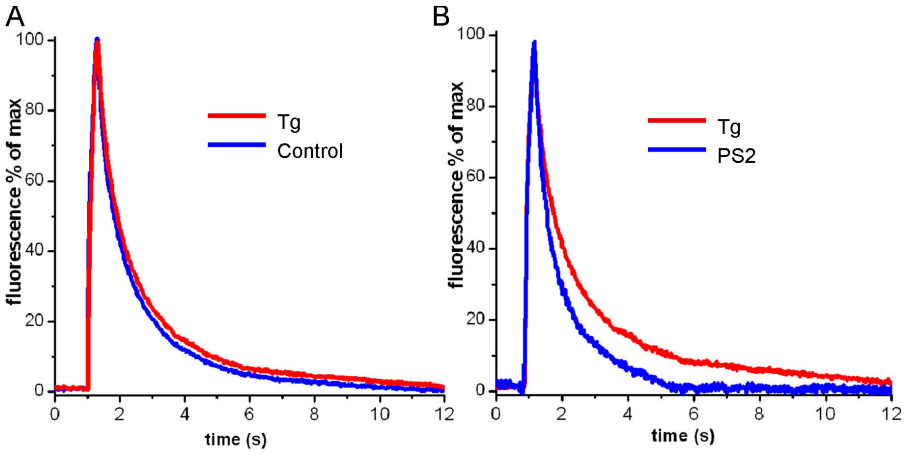

Figure 4. **Thapsigargin-sensitive cytosolic Ca^{2+} sequestration is bigger in PS2-expressing oocytes as compared with control oocytes.** (A) Traces show Ca^{2+}-dependent fluorescent signals obtained in control and PS2-expressing oocytes in the absence of (control) and during application of 30 μM thapsigargin (Tg) in the bathing solution. (B) Comparison of thapsigargin-sensitive component of cytosolic Ca^{2+} clearance in control oocytes versus PS2-expressing oocytes. Traces were obtained by direct subtraction of records obtained in the presence of 30 μM thapsigargin minus records obtained in the absence of thapsigargin. (C) Table listing fast (T1) and slow (T2) time constants of double-exponential fits to the Ca^{2+} decay data.

C **Curve fitted 2nd Order rates of decay**

	T1 (s)	T2 (s)
Control	0.567	2.471
Control + Tg	0.715	3.687
PS2	0.258	1.339
PS2 + Tg	0.550	3.263

influx through open nicotinic channels. The decay rate of the fluorescence signals after termination of the voltage pulse was then used to quantify the rate of Ca^{2+} sequestration from the cytosol. For video footage of Ca^{2+} entry and subsequent clearance from the cytosol in this system please see Video 1 (available at http://www.jcb.org/cgi/content/full/jcb.200706171/DC1).

Fig. 3 A shows mean traces of Oregon Green fluorescence, illustrating differences in the decay rate of the Ca^{2+} signal in control, PS1-, PS2- and SERCA2b-expressing oocytes. The decay presumably reflects a summation of several factors (e.g., diffusion of Ca^{2+} ions into the interior of the oocyte, mitochondrial uptake, and extrusion across the plasma membrane) in addition to sequestration into the ER by SERCA pumps. Consistent with this, decay kinetics were best fit by double-exponential processes (Fig. 2, B–D), with time constants of a few hundred milliseconds and a few seconds (Fig. 2 E). Sequestration by SERCA pumps is expected to be reflected primarily in the slower component (τ2) and, in agreement with this interpretation, τ2 was accelerated almost twofold in SERCA2b-overexpressing oocytes as compared with control cells.

The acceleration of Ca^{2+} sequestration was even greater in oocytes expressing PS2 than in those overexpressing SERCA2b, and a small acceleration was also evident with overexpression of PS1 (Fig. 3 E). These results confirm our finding that PS2 plays a more important role in regulating ER store Ca^{2+} refilling than does PS1 (Fig. 1), and they point to regulatory roles in both mammalian cells and *X. laevis* oocytes.

Pharmacological inhibition of SERCA prevents presenilin-mediated acceleration of cytosolic Ca^{2+} sequestration

Overexpression of either PS1, 2, or SERCA resulted in an accelerated sequestration of the cytosolic Ca^{2+} after a controlled Ca^{2+} influx across the plasma membrane, with PS2 having the most robust effect (Fig. 3). To prove that overexpression of presenilin was accelerating Ca^{2+} clearance from the cytosol by increasing SERCA activity, we measured Ca^{2+} clearance in the presence of thapsigargin, a specific inhibitor of SERCA. If our hypothesis was true, then presenilin should no longer accelerate clearance of Ca^{2+} from the cytosol in the presence of thapsigargin, compared with control oocytes also in the presence of thapsigargin. We incubated control and PS2-expressing oocytes in 30 μM thapsigargin in the bathing solution for 30 min. After a 30-min incubation, we applied a 300-ms hyperpolarization pulse, as before, to allow a controlled influx of Ca^{2+} across the plasma membrane into the cytosol and then tracked the clearance of this Ca^{2+} into the intracellular stores. In both control and PS2-expressing oocytes, thapsigargin reduced the speed of the Ca^{2+} fluorescence decay, with PS2-expressing oocytes showing the strongest effect, which is consistent with impairment of PS2 modulation of SERCA activity (Fig. 4, A and B). Double-exponential curve fitting revealed that both control and PS2-expressing oocytes had similar τ1 and τ2 values, despite PS2-overexpressing oocytes having markedly faster τ2 values compared with control oocytes in the absence of thapsigargin (Fig. 4 C).

PS1 familial AD (FAD) mutation M146V accelerates cytosolic Ca^{2+} sequestration

Mutations in the presenilins have been associated with enhanced IP_3-mediated Ca^{2+} release from oocytes (Leissring et al., 1999a,b) and a variety of mammalian cell types (Smith et al., 2002). We have showed that wild-type presenilins accelerate Ca^{2+} sequestration from the cytosol in a thapsigargin-sensitive pathway and that overexpression of SERCA phenocopies this. We expressed the presenilin FAD mutant PS1M146V in *X. laevis*

A

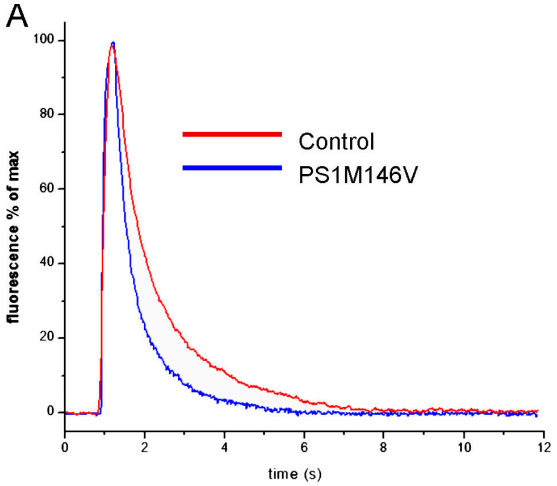

B **Curve fitted 2nd Order rates of decay**

	T1 (s)	T2 (s)
Control	0.580	2.519
PS1M146V	0.276	1.114

Figure 5. **PS1 FAD mutation M146V accelerates cytosolic Ca^{2+} sequestration.** (A) Traces show Ca^{2+}-dependent fluorescence changes ($\Delta F/F_o$) after 300-ms hyperpolarizing pulses to induce Ca^{2+} entry through nAChR expressed in the plasma membrane obtained from control and PS1 M146V expressing oocytes. (B) Table listing fast (T1) and slow (T2) time constants of double-exponential fits to the Ca^{2+} decay data.

oocyte and recorded cytosolic Ca^{2+} decay after a 300-ms Ca^{2+} influx through the nAChR as before. The Ca^{2+} decay was substantially accelerated in oocytes expressing PS1M146V compared with control (Fig. 5 A). Double-exponential curve fitting revealed substantial acceleration in both $\tau 1$ and $\tau 2$ components with PS1M146V over control (Fig. 5 B). Rates of decay were faster than wild-type PS1 expression alone ($\tau 1$, 0.373 vs. 0.276; $\tau 2$, 1.919 vs. 1.114), suggesting that this mutation impacts Ca^{2+} cytosolic sequestration more effectively than wild-type PS1 protein.

SERCA2b overexpression increases IP_3-mediated calcium release

We previously showed that overexpression of either PS1 or PS2 leads to an increase in IP_3-mediated Ca^{2+} release in *X. laevis* oocytes (Leissring et al., 1999a,b), but it was unclear whether this arose through increased activation or conductance of IP_3 receptor/channels or from enhanced store filling. To discriminate between these possibilities, we examined whether enhanced SERCA pump activity could replicate the increased IP_3 response. We monitored Ca^{2+} liberation by linescan confocal microscopy in response to photorelease of IP_3 from a caged precursor evoked by UV flashes of varying duration as previously described (Leissring et al., 1999a,b). Similar to the effects of presenilin overexpression, mean Ca^{2+} responses evoked by high IP_3 were enhanced by ~50% (Fig. 6 D), and the decay of IP_3-evoked Ca^{2+} transients was accelerated (Figs. 6, B and C). These findings show that an increase in SERCA pump activity mimics the phenotype previously seen with presenilin overexpression.

SERCA2b and PS1/PS2 are colocalized and interact

Although both PS1 and PS2 have been localized to ER in several cell types (Walter et al., 1996) and SERCA is an ER Ca^{2+} pump, it is not known if they colocalize within specific regions of the ER. To address this question, we used confocal dual-label imaging of wild-type fibroblasts using a polyclonal antiserum against SERCA2b and a polyclonal antiserum against either PS1 or PS2 and found that SERCA2b and PS2 do colocalize, whereas colocalization between SERCA2b and PS1 was present but not as prevalent (Fig. 7 A).

To biochemically determine whether presenilins physically associate with SERCA2b, we conducted immunoprecipitation experiments. Fibroblast cell lysates were immunoprecipitated with either a PS1- or PS2-specific antibody or an irrelevant control antibody (anti-p35). The resultant pellets were fractionated on a 4–12% Bis/Tris gel and immunoblotted for SERCA2b. Both PS1 and PS2 were found to specifically bind to SERCA2b, whereas SERCA2b did not coprecipitate with the control antibody (Fig. 7 B). Conversely, immunoprecipitating with an anti-SERCA2b antibody followed by immunoblotting for PS1 or PS2 was not feasible because the weights of the IgG heavy and light chains (~55 and 25 kD) are the same as of presenilin holoprotein (~55 kD) or carboxy fragment (~22 kD), and although using different species of polyclonal antibodies revealed bands at the correct weights, we could not absolutely determine whether they were presenilin or cross-reactivity with intraspecies IgG chains.

SERCA activity regulates Aβ production

Our data indicate that presenilins are required for normal SERCA function and physiological maintenance of cellular calcium homeostasis. Moreover, given that presenilins are integral for the production of Aβ, we investigated whether SERCA function influenced Aβ production. To address this issue, we used pharmacological and gain-of-function and loss-of-function genetic approaches. First, we considered the consequences of overexpressing SERCA2b in CHO cells stably expressing APP. After 48 h, we found that higher SERCA2b levels caused a marked increase in Aβ40 production (Fig. 8 A). Conversely, reducing SERCA2b via siRNA-mediated knockdown caused a significant decrease in both Aβ40 and Aβ42 levels (Fig. 8 B). Pharmacological inhibition of SERCA2b with thapsigargin rapidly reduced Aβ40 and Aβ42 production (Fig. 8, C and D), which is in agreement with SERCA2b knockdown. The sum of these findings indicates that SERCA pump activity impacts Aβ production.

Discussion

Cellular Ca^{2+} dyshomeostasis has been consistently observed in numerous experimental systems harboring presenilin mutations, including *X. laevis* oocytes, transfected cell lines, genetically altered mice, and human fibroblasts from FAD patients (LaFerla, 2002). These pathological disruptions in Ca^{2+} signaling suggest that the presenilins may play a physiological role in cellular Ca^{2+} regulation, although this has not been firmly established or characterized. In this paper, we examined the role of wild-type presenilins

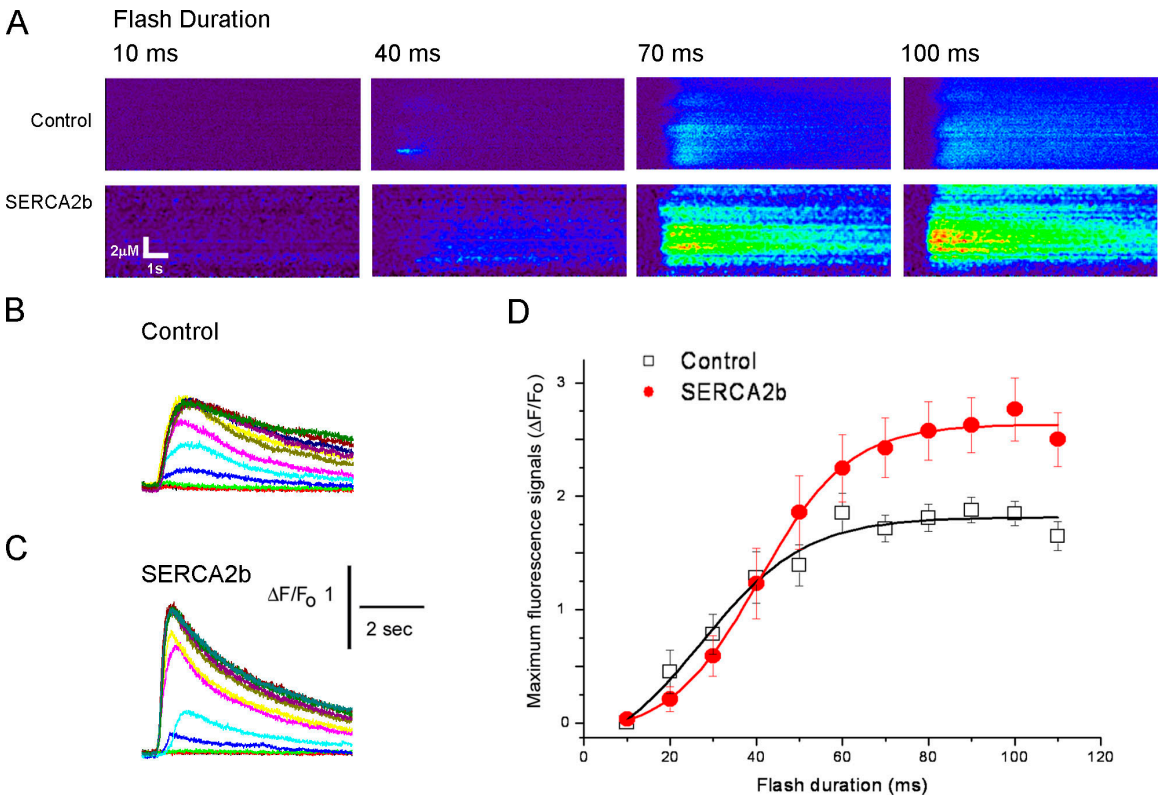

Figure 6. **Overexpression of SERCA2b phenocopies the enhanced IP_3-evoked signals and accelerated Ca^{2+} decay observed with presenilin overexpression.** (A) Representative linescan images showing Ca^{2+} signals evoked by photolysis flashes of 10-, 40-, 70-, and 100-ms durations. In each panel, distance along the scan line is depicted vertically, time runs from left to right, and increasing fluorescence ratio (increasing Ca^{2+}) corresponds to increasingly "warm" colors. Note the enhanced response in the oocyte overexpressing SERCA2b. (B and C) B and C show, respectively, Ca^{2+}-dependent fluorescence signals evoked by photoreleased IP_3 in a control oocyte and an oocyte expressing SERCA2b. In each panel, superimposed traces show responses (fluorescence ratio change averaged across the scan line) evoked by UV light flash durations in 10-ms increments between 10 and 110 ms. (D) Mean peak Ca^{2+} concentration plotted as a function of flash duration (linearly proportional to IP_3) in control oocytes (n = 6) and in oocytes expressing SERCA2b (n = 5) from at least six recordings from multiple oocytes. Error bars show SEM.

on Ca^{2+} regulation in a mammalian cell system by using genetic knockout models and also in *X. laevis* oocytes through protein overexpression. Our results indicate that the presenilins regulate the activity of the SERCA pump and are necessary for its proper functioning. Indeed, siRNA knockdown of SERCA leads to a phenotype resembling presenilin-null cells (Fig. 1 A vs. Fig. 2 F), including elevated basal Ca^{2+} levels (also seen in Zhang et al. [2006]) and diminished thapsigargin-mediated Ca^{2+} release. Altered cytosolic Ca^{2+} levels probably arise because of changes in other Ca^{2+} influx pathways as a result of SERCA down-regulation, as it is unlikely that SERCA directly controls basal cytosolic Ca^{2+}. However, both of these phenotypes in presenilin-null cells are rescued by overexpression of presenilin (Fig. 2 A). Although interpretation of our functional data in cell lines is dependent on Ca^{2+} rises evoked by thapsigargin, which has pitfalls associated with it, the data obtained in oocytes confirm presenilin as a positive modulator of SERCA function. Overexpression of presenilins accelerates the clearance of a known quantity of Ca^{2+} from the cytosol with similar dynamics to SERCA overexpression. Crucially, accelerated Ca^{2+} clearance with presenilin overexpression is prevented by pharmacological inhibition of SERCA, providing direct functional evidence for an interaction between presenilin and SERCA. Supporting a physiological role for the presenilins, a recent study suggested that they can form Ca^{2+} leak channels in the ER (Tu et al., 2006) and are an integral part of intracellular Ca^{2+} homeostasis via passive leak from the ER stores. The prospect of presenilins forming ER leak channels is, however, at odds with the observation that overexpression of presenilins leads to enhanced IP_3-mediated Ca^{2+} release (Leissring et al., 1999a,b; Smith et al., 2002). Wild-type presenilin should increase passive leak from the ER stores, resulting in diminished IP_3-mediated Ca^{2+} release, whereas the opposite actually occurs, with FAD-linked presenilin mutations augmenting IP_3-mediated Ca^{2+} release even further (Leissring et al., 1999a,b). This paradox suggests that presenilins also have an impact on Ca^{2+} homeostasis through other means, which should be sufficient to explain how wild-type presenilin overexpression enhances IP_3-mediated responses, whereas presenilin knockout cells have reduced IP_3-mediated responses (Leissring et al., 2002). Presenilin regulating SERCA function is consistent with both of these observations, as we have shown in both mammalian cell lines and *X. laevis* oocyte expression systems, with overexpression of SERCA resulting in enhanced IP_3-mediated Ca^{2+} release mimicking the phenotype seen with overexpression of presenilin (Fig. 5). Combining this with our data, it appears that presenilins contribute to both the active filling of the ER stores and the passive emptying and helps explain why mutations in these proteins have such widespread effects on global Ca^{2+} signaling.

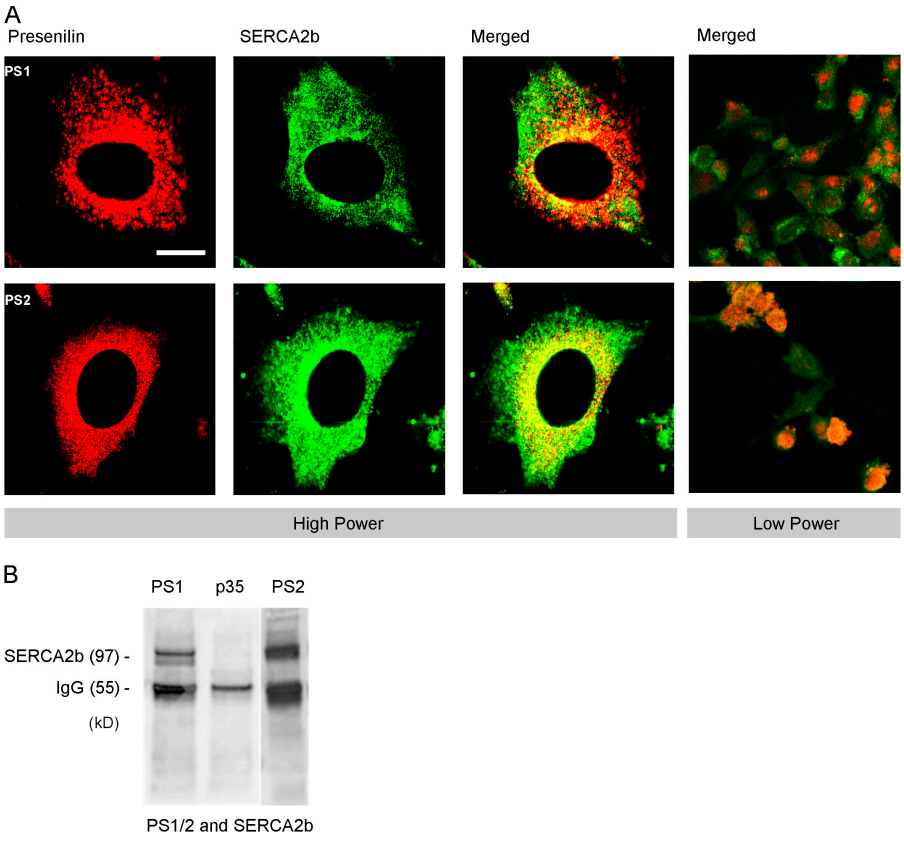

Figure 7. **Colocalization of presenilin and SERCA2b.** (A) Confocal images of fibroblasts showing dual staining for PS1 or PS2 (red) together with SERCA2b (green). Merged images with sites of colocalization in yellow are shown on the right. (B) Western blots show coimmunoprecipitation of SERCA2b with PS1 and PS2 in fibroblast cell lysates. Polyclonal rabbit anti-PS1 or -PS2 antibodies were used to immunoprecipitate SERCA2b, which was then detected using anti-SERCA2b antibody. No SERCA2b immunoprecipitation was apparent with a control (rabbit polyclonal anti-p35) antibody. Bar, 10 μm.

As both presenilin and SERCA have activities that can be modulated by several proteins as well as by one another, this presents an interesting question: if presenilins regulate SERCA function, then can SERCA also regulate γ-secretase activity? Several studies have illustrated how modulating Ca^{2+} influx can modulate production of the Aβ peptide (Querfurth and Selkoe, 1994; Pierrot et al., 2004), as well as increasing intracellular store release (Querfurth et al., 1997). Indeed, any regimen that affects intracellular Ca^{2+} will invariably alter the activity of SERCA, as it is itself modulated by cytosolic and ER Ca^{2+} concentration as models have shown (Yano et al., 2004). In this paper, we demonstrate through both pharmacological and genetic means that modulation of SERCA2b function results in altered Aβ production with decreased SERCA function leading to decreased Aβ and increased SERCA function leading to increased Aβ. Therefore, it seems possible that SERCA activity plays a modulatory role in γ-secretase function or at least in APP processing leading to further generation of the Aβ peptide. Curiously, it has been reported that either stimulation (Pierrot et al., 2004) or inhibition (Yoo et al., 2000) of capacitative Ca^{2+} entrance (CCE) leads to increased production of $Aβ_{42}$. Our results show that thapsigargin treatment, which depletes ER stores, diminishes

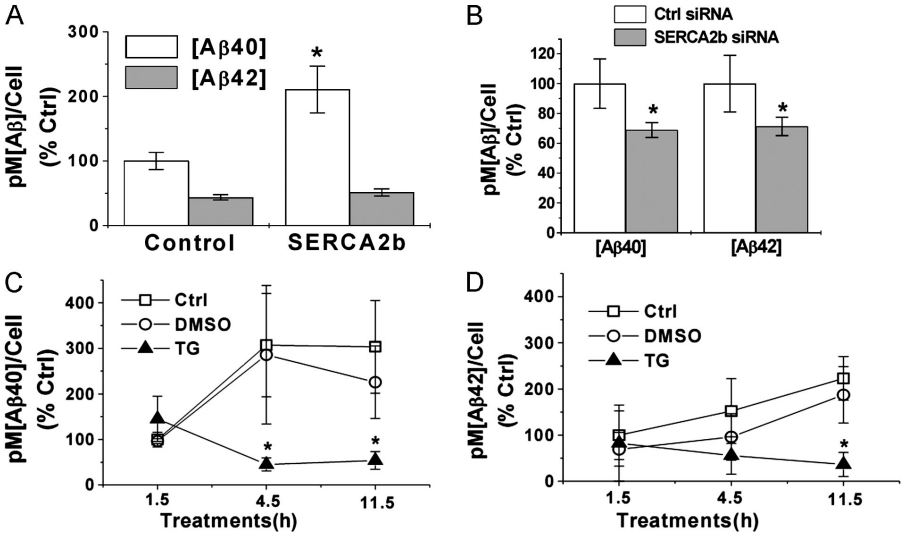

Figure 8. **SERCA activity regulates Aβ production.** (A) SERCA2b overexpression leads to higher Aβ levels. Aβ40 and Aβ42 levels were measured by sandwich ELISA. Note that Aβ40 levels are significantly increased in SERCA2b-transfected cells, compared with control pcDNA vector-treated cells (*, $P < 0.05$; $n = 5$). (B) Genetic down-regulation of SERCA2b expression lowers Aβ levels. siRNA-mediated down-regulation of SERCA2b leads to lower steady-state Aβ levels when compared with cells treated with a control (scrambled) siRNA (*, $P < 0.05$; $n = 6$). (C and D) Pharmacological inhibition of SERCA activity lowers steady-state Aβ levels. Inhibition of SERCA2b with 1 μM thapsigargin in the presence of extracellular Ca^{2+} decreases Aβ40 levels within 4.5 h ($n = 4$) and also decreases Aβ42 levels within 11.5 h ($n = 4$). 4.5 h: *, $P < 0.005$ for thapsigargin and control; *, $P < 0.05$ for thapsigargin and DMSO. 11.5 h: *, $P < 0.005$ for thapsigargin and control; *, $P < 0.05$ for thapsigargin and DMSO. Error bars show SEM.

Aβ production, yet depletion of ER stores leads to increased Ca^{2+} influx via CCE. This suggests that depleting ER stores of Ca^{2+} has a stronger effect on preventing Aβ production than CCE activation has on inhibiting it.

Numerous proteins, such as calsenilin, ryanodine receptor, and calmyrin (for review see Chen and Schubert, 2002), have been shown to interact with and bind the presenilins as well as the known components of the γ-secretase complex (nicastrin, PEN2, and Aph1), making the presenilins part of a very large multiprotein complex with multiple functions. Our results suggest that the interaction between SERCA and presenilin is an additional, but very important, interaction that serves to regulate sequestration of calcium into the ER stores, making presenilin a key component of cellular calcium homeostasis. A puzzling aspect is how mutations in the presenilins that modulate γ-secretase activity could cause the increases in intracellular Ca^{2+} signaling reported (Leissring et al., 1999a,b). Conversely, inhibitors of γ-secretase, which bind to the active site of presenilin in the γ-secretase complex, completely diminish ER Ca^{2+} release (Leissring et al., 2002; Kasri et al., 2006). Mutations in presenilin have been reported to disrupt the formation of ER leak channels, thereby preventing passive Ca^{2+} leak, which then leads to store overfilling (Tu et al., 2006) and, hence, exaggerated IP_3-mediated release. Whether these same mutations also affect presenilins' modulation of SERCA function remains to be seen, but many of these FAD-linked mutations are associated with an increase, or at least change, in γ-secretase activity, making the prospect plausible. Indeed, we have shown here that the FAD-linked PS1 mutation M146V does show enhanced clearance of cytosolic Ca^{2+} compared with wild-type PS1. The requirement of SERCA activity to have presenilins present may provide problems for drugs that inhibit the actions of the γ-secretase complex to therapeutically reduced Aβ levels in AD. Such drugs have already been shown to abolish ER Ca^{2+} release in cell cultures (Leissring et al., 2002; Kasri et al., 2006) but their chronic in vivo use has yet to be documented. Certainly, reducing or abolishing ER Ca^{2+} release in neurons will have massive implications on memory and behavior, which suggests that BACE may be a more prudent drug target to reduce Aβ in AD.

Materials and methods

Cell culture and calcium imaging

MEFs (Bart de Strooper, Katholieke Universiteit Leuven, Leuven, Netherlands) and CHO cells were maintained with DME and 10% FBS. Calcium imaging was performed as previously described (Leissring et al., 2002). In brief, measurements of intracellular calcium were obtained using the InCyt Im2 Ration imaging system (Intracellular Imaging, Inc.) using excitation at 340 and 380 nm. cDNA transfection was achieved using the Nucleofection technique (Amaxa) as per the manufacturer's instructions. 5 µg cDNA was used alongside 1 µg GFP cDNA to assess transfection efficiency and for selecting cells that had been successfully transfected for Ca^{2+} imaging. Typically, 70% transfection efficiency was seen.

RNA interference

A 20:1 stock solution of opti-MEM (Invitrogen) to Mirus TransIT-LT1 transfection reagent (Mirus Bio) was incubated at room temperature for 20 min. siRNAs were added and the solution was incubated for an additional 20 min at room temperature. This mixture was then added to cells, already in opti-MEM, to a final siRNA concentration of 25 nM of each partial sequence. The cells were then incubated in 5% CO_2 atmosphere at 37°C for 12 h. Subsequently, cells were rescued with DME containing 10% FBS for an additional 12 h in 5% CO_2 atmosphere at 37°C. Thereafter, cells were given the same siRNA treatment for an additional 12 h and rescued for the next 12 h with DME containing 10% FBS in 5% CO_2 atmosphere at 37°C. Cells were then lysed and the lysates were stored at −80°C for further immunoblotting analysis. SERCA2b siRNA was acquired as a smartpool containing the following partial sequences: GUCAAUGUCGGUUU, CAAAGUUCCUGCUG, GAUCAUGUCUGUCA, and GAUAUAAGGUUAAC.

Oocyte calcium imaging and photolysis of caged IP_3

Plasmids containing cDNA clones encoding for human PS1, PS2, SERCA2b, and the mouse muscle α, β, γ, and δ nAChR subunits (S.F. Heinemann, Salk Institute, La Jolla, CA) were linearized and transcribed in vitro with SP6 or T3 RNA polymerases as previously described (Leissring et al. 1999b). The RNA transcripts were extracted with phenol-chloroform, precipitated with ethanol, and suspended in RNase-free water at a concentration of 1 µg/µl.

Defolliculated stage-VI oocytes from *X. laevis* were prepared as previously described (Demuro et al. 2005) and injected the next day with 46 nl of the appropriate cRNA mixtures. 3 d after cRNA injection and 1–4 h before Ca^{2+} imaging experiments, oocytes were injected with 23 nl of 2 mM of Oregon Green BAPTA-1 (Invitrogen) alone or together with 0.5 mM of caged Ins(1,4,5)P_3 (D-myo-inositol 1,4,5-trisphosphate $P^{4(5)}$-{1-(2-nitrophenyl)ethyl]ester; Invitrogen) for experiments involving IP_3-mediated Ca^{2+} release.

For experiments imaging the clearance of Ca^{2+} after plasma membrane influx (Fig. 3), oocytes were voltage clamped using a conventional two-microelectrodes technique. The membrane potential was held at 0 mV during superfusion with ACh (100–500 nM) in Ringer's solution and was briefly (300 ms) stepped to −150 mV to strongly increase the electrical driving force for Ca^{2+} influx. Oocytes were imaged at room temperature by wide-field fluorescence microscopy using an inverted microscope (IX 71; Olympus) equipped with a 60× oil-immersion objective, a 488-nm argon-ion laser for fluorescence excitation, and a charge-coupled device camera (Cascade 128+; Roper Scientific) for imaging fluorescence emission (510–600 nm) at frame rates of up to 500 s^{-1}. Fluorescence signals were monitored from a 40 × 40-µm region within the animal hemisphere of the oocyte and are expressed as a ratio ($\Delta F/F_o$) of the mean change in fluorescence (ΔF) relative to the resting fluorescence before stimulation (F_o) using MetaMorph software (MDS Analytical Technologies). Mean values of F_o were obtained by averaging over several frame before stimulation.

Experiments measuring Ca^{2+} liberation in response to photolysis of caged IP_3 (Fig. 4) were performed using a linescan confocal microscope (IX-70 inverted microscope with a 40× oil-immersion fluor objective lens, using a 488-nm beam from a 100-mW argon laser [Callamaras and Parker, 1999]) to image fluorescence signals evoked by flashes of UV light (340–400 nm) from a mercury arc lamp, illuminating a disc of 100-µm diameter surrounding the 50-µm scan line in the animal hemisphere of the oocyte.

Protein immunoblotting

Protein extracts were prepared from cells using M-per (Thermo Fisher Scientific) extraction buffer and Complete Mini Protease Inhibitor Tablets (Roche). Protein concentrations were determined by the Bradford method. Equal amounts of protein (10 µg) were separated by SDS/PAGE on a 4–12% Bis/Tris gel (Invitrogen), transferred to PDVF membranes, blocked for 1 h in 5% vol/vol nonfat milk in Tris-buffered saline, pH 7.5, supplemented with 0.2% Tween 20, and incubated overnight at 4°C with primary antibody. Antibodies and dilutions used in this study include α-SERCA2b (1:20,000; F. Wuytack, Katholieke Universiteit Leuven, Leuven, Netherlands), CTF20 (1:5,000; EMD), and α-Actin (1:10,000; Sigma-Aldrich). Membranes were washed five times and then incubated with HRP-conjugated secondary antibodies for 1 h at room temperature. Quantitative densitometric analyses were performed on digitized images of immunoblots with Scion Image 4.0 (Scion Corporation).

Aβ ELISA

MaxiSorp immunoplates (Thermo Fisher Scientific) were coated with BAN50 at a concentration of 5 µg/ml in 0.1 M NaCO3 buffer, pH 9.6, and blocked with 1% Block Ace (Snow Brand Milk Products, Ltd.). Synthetic Aβ standards, internal controls, and samples were run at least in duplicate. After overnight incubation at 4°C, wells were probed with either HRP-conjugated BA27 (for Aβ1-40) or BC05 (for Aβ1-42) for 2–3 h at 37°C. 3,3′,5,5′-tetramethylbenzidine was used as the chromogen, and the reaction

was stopped by 6% *O*-phosphoric acid and read at 450 nm on a plate reader (Molecular Dynamics). Data are reported as mean per live cell + SEM, and statistical significance was evaluated using Student's *t* test.

Immunoprecipitation

50 µg MEF cell lysate was incubated with 40 µl of Protein A Sepharose beads (Sigma-Aldrich) for 1 h and centrifuged, and the supernatant was recovered. A further 40 µl of beads was added along with anti-PS1 (Cell Signaling Technology), PS2 (G. Thinakaran, University of Chicago, Chicago, IL), or p35 (Santa Cruz Biotechnology, Inc.) as a control (1:100), and the volume was made up to 1 ml with water and incubated overnight at 4°C overnight. After pelleting the beads, the supernatant was discarded and the beads were washed with STEN buffer (0.15 M NaCl, 0.05 M Tris HCl, 0.002 M EDTA, and 2% NP-40, pH 7.6) and then STEN containing 0.1% SDS. The beads were then pelleted and 4× loading buffer was added (Invitrogen). The samples were boiled for 10 min and spun down again, and the supernatant was run on a 4–12% Bis/Tris gel. SERCA2b was probed using αSERCA2b (1:20,000; F. Wuytack).

Confocal microscopy

Fluorescent immunolabeling followed a standard two-way technique (primary antibody followed by fluorescent secondary antibody). Free-floating sections were rinsed in TBS, pH 7.4, and then blocked (0.25% Triton X-100 and 5% normal goat serum in TBS) for 1 h. Sections were incubated in primary antibody overnight at 4°C, rinsed in PBS, and incubated for 1 h in either fluorescently labeled anti–rabbit or anti–mouse secondary antibodies (Alexa 488, 1:200; Invitrogen). Confocal images were captured on a confocal system (Radiance 2100;Bio-Rad Laboratories). All double-labeled specimens were imaged using the λ-strobing function to prevent nonspecific cross-excitation of fluorophores.

Statistics

Data are presented as mean ± 1 SEM, with n = number of cells examined. An unpaired Student's *t* test was used to determine statistical significance ($P < 0.05$).

Online supplemental material

Video 1 shows representative calcium clearance from oocyte cytosol after a 300-ms influx through nAChR. Online supplemental material is available at http://www.jcb.org/cgi/content/full/jcb.200706171/DC1.

We thank Dr. Bart de Strooper for the PS knockout fibroblasts, Dr. Frank Wuytack for the generous gift of the anti-SERCA2b antibody, and Dr. Gopal Thinakaran for providing us with the anti-PS2 antibody. We are also grateful to Dr. Stephen F. Heinemann for providing the muscle nAChRs subunits cDNAs.

This work was supported by the National Institutes of Health (grants AG17968, AG16573, and GM48071).

Submitted: 26 June 2007
Accepted: 28 May 2008

References

Aubier, M., and N. Viires. 1998. Calcium ATPase and respiratory muscle function. *Eur. Respir. J.* 11:758–766.

Baba-Aissa, F., L. Raeymaekers, F. Wuytack, L. Dode, and R. Casteels. 1998. Distribution and isoform diversity of the organellar Ca2+ pumps in the brain. *Mol. Chem. Neuropathol.* 33:199–208.

Berridge, M.J., P. Lipp, and M.D. Bootman. 2000. The versatility and universality of calcium signalling. *Nat. Rev. Mol. Cell Biol.* 1:11–21.

Callamaras, N., and I. Parker. 1999. Radial localization of inositol 1,4,5-trisphosphate-sensitive Ca2+ release sites in *Xenopus* oocytes resolved by axial confocal linescan imaging. *J. Gen. Physiol.* 113:199–213.

Chen, Q., and D. Schubert. 2002. Presenilin-interacting proteins. *Expert Rev. Mol. Med.* 4:1–18.

Demuro, A., E. Mina, R. Kayed, S.C. Milton, I. Parker, and C.G. Glabe. 2005. Calcium dysregulation and membrane disruption as a ubiquitous neurotoxic mechanism of soluble amyloid oligomers. *J. Biol. Chem.* 280:17294–17300.

Duff, K., C. Eckman, C. Zehr, X. Yu, C.M. Prada, J. Perez-tur, M. Hutton, L. Buee, Y. Harigaya, D. Yager, et al. 1996. Increased amyloid-beta42(43) in brains of mice expressing mutant presenilin 1. *Nature.* 383:710–713.

Hass, M.R., and B.A. Yankner. 2005. A {gamma}-secretase-independent mechanism of signal transduction by the amyloid precursor protein. *J. Biol. Chem.* 280:36895–36904.

Herms, J., I. Schneider, I. Dewachter, N. Caluwaerts, H. Kretzschmar, and F. Van Leuven. 2003. Capacitive calcium entry is directly attenuated by mutant presenilin-1, independent of the expression of the amyloid precursor protein. *J. Biol. Chem.* 278:2484–2489.

Herreman, A., D. Hartmann, W. Annaert, P. Saftig, K. Craessaerts, L. Serneels, L. Umans, V. Schrijvers, F. Checler, H. Vanderstichele, et al. 1999. Presenilin 2 deficiency causes a mild pulmonary phenotype and no changes in amyloid precursor protein processing but enhances the embryonic lethal phenotype of presenilin 1 deficiency. *Proc. Natl. Acad. Sci. USA.* 96:11872–11877.

Kasri, N.N., S.L. Kocks, L. Verbert, S.S. Hebert, G. Callewaert, J.B. Parys, L. Missiaen, and H. De Smedt. 2006. Up-regulation of inositol 1,4,5-trisphosphate receptor type 1 is responsible for a decreased endoplasmic-reticulum Ca2+ content in presenilin double knock-out cells. *Cell Calcium.* 40:41–51.

LaFerla, F.M. 2002. Calcium dyshomeostasis and intracellular signalling in Alzheimer's disease. *Nat. Rev. Neurosci.* 3:862–872.

Leissring, M.A., I. Parker, and F.M. LaFerla. 1999a. Presenilin-2 mutations modulate amplitude and kinetics of inositol 1,4,5-trisphosphate-mediated calcium signals. *J. Biol. Chem.* 274:32535–32538.

Leissring, M.A., B.A. Paul, I. Parker, C.W. Cotman, and F.M. LaFerla. 1999b. Alzheimer's presenilin-1 mutation potentiates inositol 1,4,5-trisphosphate-mediated calcium signaling in *Xenopus* oocytes. *J. Neurochem.* 72:1061–1068.

Leissring, M.A., Y. Akbari, C.M. Fanger, M.D. Cahalan, M.P. Mattson, and F.M. LaFerla. 2000. Capacitative calcium entry deficits and elevated luminal calcium content in mutant presenilin-1 knockin mice. *J. Cell Biol.* 149:793–798.

Leissring, M.A., M.P. Murphy, T.R. Mead, Y. Akbari, M.C. Sugarman, M. Jannatipour, B. Anliker, U. Muller, P. Saftig, B. De Strooper, et al. 2002. A physiologic signaling role for the gamma -secretase-derived intracellular fragment of APP. *Proc. Natl. Acad. Sci. USA.* 99:4697–4702.

Lytton, J., M. Westlin, and M.R. Hanley. 1991. Thapsigargin inhibits the sarcoplasmic or endoplasmic reticulum Ca-ATPase family of calcium pumps. *J. Biol. Chem.* 266:17067–17071.

Pierrot, N., P. Ghisdal, A.S. Caumont, and J.N. Octave. 2004. Intraneuronal amyloid-beta1-42 production triggered by sustained increase of cytosolic calcium concentration induces neuronal death. *J. Neurochem.* 88:1140–1150.

Querfurth, H.W., and D.J. Selkoe. 1994. Calcium ionophore increases amyloid beta peptide production by cultured cells. *Biochemistry.* 33:4550–4561.

Querfurth, H.W., J. Jiang, J.D. Geiger, and D.J. Selkoe. 1997. Caffeine stimulates amyloid beta-peptide release from beta-amyloid precursor protein-transfected HEK293 cells. *J. Neurochem.* 69:1580–1591.

Smith, I.F., J.P. Boyle, P.F. Vaughan, H.A. Pearson, R.F. Cowburn, and C.S. Peers. 2002. Ca(2+) stores and capacitative Ca(2+) entry in human neuroblastoma (SH-SY5Y) cells expressing a familial Alzheimer's disease presenilin-1 mutation. *Brain Res.* 949:105–111.

Stutzmann, G.E., A. Caccamo, F.M. LaFerla, and I. Parker. 2004. Dysregulated IP3 signaling in cortical neurons of knock-in mice expressing an Alzheimer's-linked mutation in presenilin1 results in exaggerated Ca2+ signals and altered membrane excitability. *J. Neurosci.* 24:508–513.

Tu, H., O. Nelson, A. Bezprozvanny, Z. Wang, S.F. Lee, Y.H. Hao, L. Serneels, B. De Strooper, G. Yu, and I. Bezprozvanny. 2006. Presenilins form ER Ca2+ leak channels, a function disrupted by familial Alzheimer's disease-linked mutations. *Cell.* 126:981–993.

Walter, J., A. Capell, J. Grunberg, B. Pesold, A. Schindzielorz, R. Prior, M.B. Podlisny, P. Fraser, P.S. Hyslop, D.J. Selkoe, and C. Haass. 1996. The Alzheimer's disease-associated presenilins are differentially phosphorylated proteins located predominantly within the endoplasmic reticulum. *Mol. Med.* 2:673–691.

Yano, K., O.H. Petersen, and A.V. Tepikin. 2004. Dual sensitivity of sarcoplasmic/endoplasmic Ca2+-ATPase to cytosolic and endoplasmic reticulum Ca2+ as a mechanism of modulating cytosolic Ca2+ oscillations. *Biochem. J.* 383:353–360.

Yoo, A.S., I. Cheng, S. Chung, T.Z. Grenfell, H. Lee, E. Pack-Chung, M. Handler, J. Shen, W. Xia, G. Tesco, et al. 2000. Presenilin-mediated modulation of capacitative calcium entry. *Neuron.* 27:561–572.

Zhang, S.L., A.V. Yeromin, X.H. Zhang, Y. Yu, O. Safrina, A. Penna, J. Roos, K.A. Stauderman, and M.D. Cahalan. 2006. Genome-wide RNAi screen of Ca(2+) influx identifies genes that regulate Ca(2+) release-activated Ca(2+) channel activity. *Proc. Natl. Acad. Sci. USA.* 103:9357–9362.

Zhang, Z., P. Nadeau, W. Song, D. Donoviel, M. Yuan, A. Bernstein, and B.A. Yankner. 2000. Presenilins are required for gamma-secretase cleavage of beta-APP and transmembrane cleavage of Notch-1. *Nat. Cell Biol.* 2:463–465.